

Effective mass of a space-charge layer on GaAs in a parallel magnetic field

E. Batke and C. W. Tu

AT&T Bell Laboratories, Murray Hill, New Jersey 07974

(Received 2 June 1986)

The effective mass of a quasi-two-dimensional electron space-charge layer on GaAs has been studied in a plasmon-resonance experiment for magnetic fields applied in the plane of the layer. An anisotropy of the effective mass induced by the parallel magnetic field is observed. For the in-plane direction perpendicular to the magnetic field the mass increases with its reciprocal depending quadratically on the magnetic field strength.

In space-charge layers on semiconductor interfaces carriers are bound by an electrostatic field F_s at the interface forming a narrow one-dimensional channel. Their motion parallel to the interface is free, but perpendicular to it, the motion is quantized in discrete energy levels, the subbands.¹ A magnetic field component B_{\parallel} parallel to the surface leads to the formation of so-called hybrid subbands.² Their nature is determined by the Lorentz force in a crossed-field configuration and depends upon the ratio of the electric and magnetic field strengths, expressed via l_F/l_B ($l_F^2 = \hbar^2/2meF_s$: electrical length; $l_B^2 = \hbar/eB$: magnetic length). Interband transitions have been studied experimentally both for the magnetic limit^{3,4} ($l_F/l_B \gg 1$) as well as for the electric limit ($l_F/l_B \ll 1$).^{5,6} In cyclotron resonance (CR) experiments it was demonstrated that the motion of the surface carriers shows two-dimensional (2D) and three-dimensional (3D) character for the electric and magnetic limit,⁷⁻⁹ respectively.

Here we are concerned with the intraband properties, in particular the effective mass of a high density electron space-charge layer on GaAs subject to a parallel magnetic field. The system of interest is a single interface modulation-doped $Al_{0.28}Ga_{0.72}As$ -GaAs heterostructure of surface charge density $N_S = (6.7 \pm 0.4) \times 10^{11} \text{ cm}^{-2}$ and mobility $180000 \text{ cm}^2/\text{Vs}$. The sample cross section is shown in Fig. 1. The in-plane motion of the electrons is studied with far-infrared transmission spectroscopy by measuring the 2D plasmon resonance in parallel magnetic fields up to 12 T. A grating coupler of periodicity a is prepared on top of the heterostructure to allow coupling of the normally incident radiation with the plasmons of wave vector $q = 2\pi m/a$ ($m = 1, 2, \dots$).¹⁰ For details about the sample preparation and geometry as well as the experimental setup and technique we refer the reader to Ref. 11.

The 2D plasmon dispersion in the local approach, which correctly describes the experimental situation, is related to the plasmon wave vector q and the plasmon-mass m_p by the expression¹²

$$\omega_p^2 = \frac{N_s e^2 q}{2m_p \bar{\epsilon}(\omega, q) \epsilon_0} \quad (1)$$

$\bar{\epsilon}(\omega, q)$ is an effective dielectric function depending on the geometry of the sample. For our sample configuration with a screening gate (Fig. 1) it is given by

$$\bar{\epsilon}(\omega, q) = \frac{1}{2} [\epsilon_{Ga} + \langle \epsilon_{Al} \rangle \coth(qd)] \quad (2)$$

ϵ_{Ga} is the dielectric function of GaAs and $\langle \epsilon_{Al} \rangle$ the average

dielectric function of the medium (thickness d) between the top surface and the space-charge layer. The plasmon mass is related to the free parallel motion of the space-charge layer. For an anisotropic parabolic energy dispersion with effective masses m_x^* and m_y^* the reciprocal plasmon mass is given by¹³

$$\frac{1}{m_p} = \frac{1}{m_x^*} \cos^2 \phi + \frac{1}{m_y^*} \sin^2 \phi \quad (3)$$

ϕ and $(90^\circ - \phi)$ are the angles in the plane between the wave vector q and the principal directions of the electron momentum k_x and k_y , respectively. Thus, from studies of the orientational dependence of the plasmon resonance, the effective band-structure masses can be extracted.

In Fig. 2 experimental plasmon resonances are shown for finite and zero parallel magnetic field as a function of energy. The resonances were extracted by forming the relative change in transmission,

$$\frac{\Delta T}{T} = \frac{T(B_1) - T(B_2)}{T(B_1)}$$

where $T(B)$ is the magnetic-field-dependent transmission.

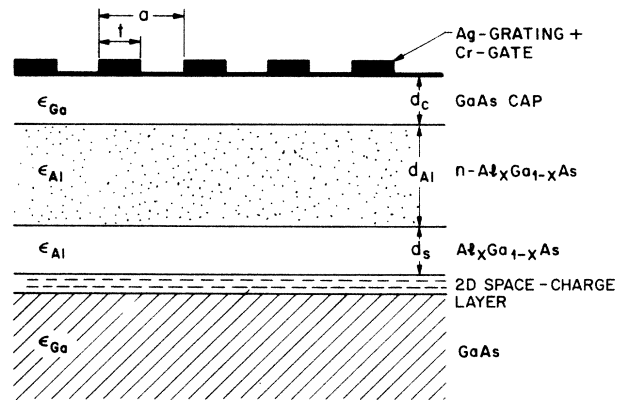


FIG. 1. Schematic sample configuration of a $Al_xGa_{1-x}As$ -GaAs heterostructure with a semitransparent metal (Cr) gate ($R_g = 1000 \Omega/\square$) and grating coupler on top. $a = 8720 \pm 70 \text{ \AA}$ is the grating period and t the stripe width. The medium between the top surface and the space-charge layer is a sandwich layer of undoped $Al_{0.28}Ga_{0.72}As$ (thickness $d_s = 35 \text{ \AA}$, dielectric function ϵ_{Al}), Si-doped $Al_{0.28}Ga_{0.72}As$ ($d_{Al} = 550 \text{ \AA}$, ϵ_{Al} , $n_{Si} = 1.0 \times 10^{18} \text{ cm}^{-3}$) and GaAs cap ($d_c = 230 \text{ \AA}$, ϵ_{Ga}) with total thickness $d = d_s + d_{Al} + d_c = 800 \pm 100 \text{ \AA}$.

The plasmon resonance for vanishing magnetic field [Fig. 2(a)] was obtained by taking the ratio between two spectra of zero and finite ($B_{\perp} \geq 8$ T) perpendicular magnetic field. In Fig. 2(b) the ratio of spectra of zero and finite ($B_{\parallel} = 11.9$ T) parallel magnetic field is taken with q oriented perpendicular to the in-plane field. The $\Delta T/T$

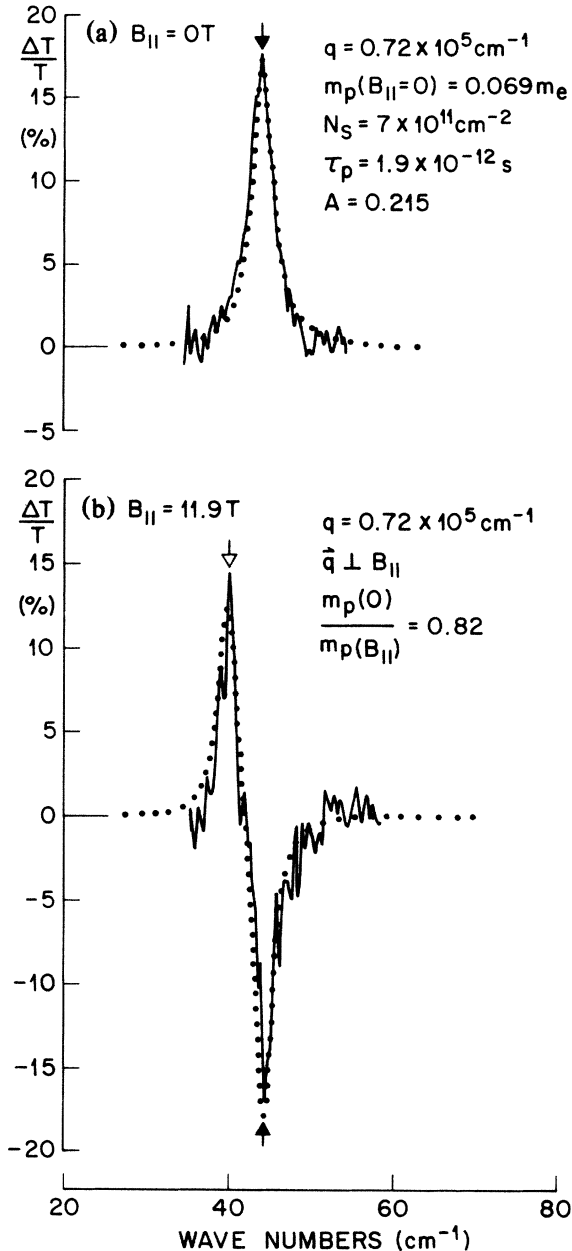


FIG. 2. 2D plasmon resonances for two different parallel magnetic field strengths. (a) $\Delta T/T$ was obtained by taking the ratio between two spectra of zero and finite perpendicular magnetic field $B_{\perp} \geq 8$ T. The dotted curve is calculated with expression (3.3) of Ref. 14 and the listed parameters. The plasmon resonance position is marked with an arrow. (b) $\Delta T/T$ was determined by taking the ratio between two spectra of zero and finite parallel magnetic field B_{\parallel} oriented perpendicular to q . The dotted curve is calculated with the same parameters as in (a) and $m_p(0)/m_p(B_{\parallel}) = 0.82$. The plasmon resonance position for $B_{\parallel} = 11.9$ T ($B_{\parallel} = 0$ T) is marked by an arrow \downarrow (\uparrow).

shown in Fig. 2(b) is a composite of two plasmon resonances with slightly different resonance positions. The resonance for finite parallel field is shifted to lower energies compared to the resonance for vanishing magnetic field. This is in contrast to a perpendicular magnetic field which shifts the 2D plasmon resonance $\omega_p(B=0$ T) by the cyclotron frequency ω_c to higher energies.¹¹

In order to determine the change of the 2D plasmon dispersion in a parallel magnetic field we studied the plasmon for $q \parallel B_{\parallel}$. In this configuration we found no structure in $\Delta T/T$ indicating that the plasmon frequency remains fixed. From this we conclude that it is the plasmon mass which is modified by an in-plane magnetic field but not N_S . Since the shift of the plasmon resonance induced by B_{\parallel} is small compared to $\omega_p(B=0$ T) and of the order of the full width at half maximum the resonance positions cannot be extracted in a simple manner from the optical spectra.

To extract the resonance positions and thus the plasmon mass from our experiment we fitted $\Delta T/T$ with an expression for T developed in Ref. 14. Apart from the plasmon dispersion the plasmon line shape is determined by the grating efficiency A and a phenomenological scattering time τ_p . The best fit to the zero field plasmon is shown in Fig. 2(a) by a dotted line and the set of parameters is listed. We substituted the plasmon mass by the cyclotron mass at low perpendicular magnetic fields $m_c = (0.0693 \pm 0.0005)m_e$. The obtained scattering time $\tau_p = 1.9 \times 10^{-12}$ s is about 3.5 times smaller than the $\tau_{dc} \approx 7 \times 10^{-12}$ s from mobility measurements. Although both scattering times are not expected to coincide, it is most likely that inhomogeneity in N_S broadens the resonances beyond τ_{dc} .¹¹ In order to obtain the resonance position for finite in-plane magnetic fields we treated the plasmon mass as an adjustable parameter. All other parameters were kept constant. The plasmon mass for $B_{\parallel} = 0$ T is known to an accuracy of about 10%, related to the uncertainties of N_S , q , ϵ_{Ga} , ϵ_{Al} , and ω_p .¹¹ Since we are determining the relative change in plasmon mass the magnetic field dependence of m_p is not affected by this particular choice of parameters. Our fit, shown in Fig. 2(b) by a dotted line, describes excellently the experimental $\Delta T/T$, and results in a relative change of the plasmon mass $m_p(0)/m_p(B_{\parallel} = 11.9$ T) = 0.82. Within our experimental accuracy we cannot establish any dependence of the scattering time on the strength of the parallel magnetic field.

In the following we compare our experimental data to theoretical work. In the electric limit the hybrid subband dispersion has been treated perturbatively.^{9,15} For an isotropic parabolic 2D system, confined in z direction and with a parallel magnetic field B_{\parallel} in y direction, the dispersion is given by¹⁵

$$E_n(k_x, k_y, B_{\parallel}) = E_n + \frac{e^2 B_{\parallel}^2 ((z_{nn}^2) - (z_{nn})^2)}{2m^*} + \frac{\hbar^2 k_y^2}{2m^*} + \frac{(\hbar k_x + eB_{\parallel} z_{nn})^2}{2m^*} + \frac{\hbar^2 e^2 B_{\parallel}^2}{m^{*2}} k_x^2 \sum_{i \neq n} \frac{|z_{in}|^2}{E_n - E_i}, \quad (4)$$

where $z_{ij}^p = \langle \phi_i(z) | z^p | \phi_j(z) \rangle$. E_n are the subband energies with associated wave functions $\phi_n(z)$ in the absence of a magnetic field. Equation (4) describes an anisotropic parabolic energy dispersion shifted in k_x direction. Thus the plasmon mass measured parallel and perpendicular to B_{\parallel} gives the effective masses of the system [see Eq. (3)]. The second expression on the right-hand side of (4) is a diamagnetic term which solely causes an upward shift of the subband energies E_n but does not affect the effective mass. The third and the last terms establish the effective masses parallel and perpendicular to the in-plane magnetic field, respectively. The latter lifts the degeneracy $E(k_x) = E(-k_x)$ which is valid in the absence of a parallel magnetic field. The theory predicts no change in the mass for $\mathbf{q} \parallel \mathbf{B}_{\parallel}$ which agrees with the experiment. For $\mathbf{q} \perp \mathbf{B}_{\parallel}$, Eq. (4) predicts a decrease of the relative reciprocal plasmon mass scaling quadratic with the parallel magnetic field strength

$$\frac{m_p(0)}{m_p(B_{\parallel})} = 1 - aB_{\parallel}^2,$$

where

$$a = \frac{2e^2}{m_p(0)} \sum_{n \geq 1} \frac{|z_{n0}|^2}{|E_n - E_0|}.$$

The decrease is caused by the last term of Eq. (4) which couples the in-plane motion of the electrons to their quantized states of the perpendicular motion. To test the theoretical field dependence we have plotted in Fig. 3 the experimental values for $m_p(0)/m_p(B_{\parallel})$ as a function of B_{\parallel}^2 . All experimental points fall on a straight line with a slope of $(1.20 \pm 0.15) \times 10^{-3} \text{ T}^{-2}$. If we assume two confined states E_0 and E_1 in the channel we can estimate the matrix element $|z_{01}|$ from this slope. Intersubband resonance experiments¹¹ on this sample show a subband separation, $|E_1 - E_0|$, of $35 \pm 5 \text{ meV}$, and we extract $|z_{01}| \approx 29 \pm 5 \text{ \AA}$. Our calculation might be rather coarse, because more than two bound states might be present in the channel. A self-consistent calculation of the subband energies and wave functions is necessary for a quantitative analysis. We hope our data will stimulate such a calculation, which could also give information on the conduction band offset

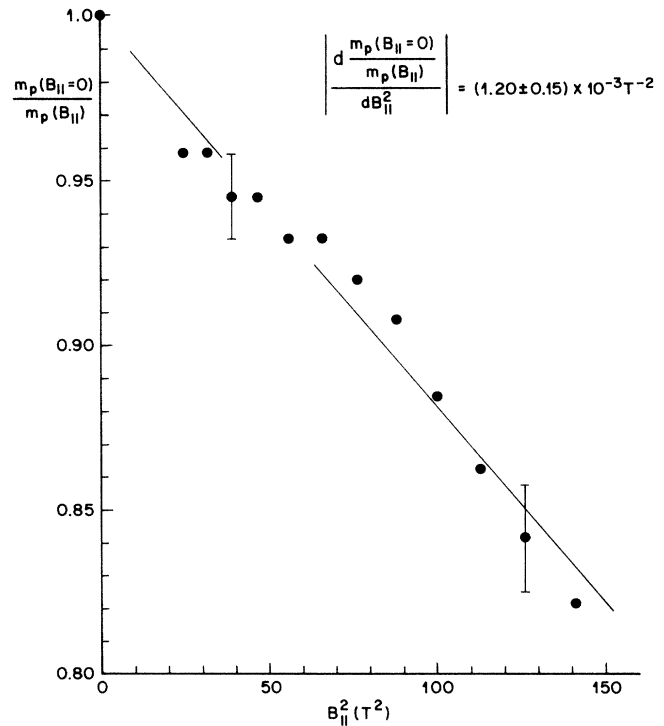


FIG. 3. Relative reciprocal plasmon mass vs the square of the parallel magnetic field strength B_{\parallel}^2 . The straight line is a guide to the eye.

between GaAs and $\text{Al}_x\text{Ga}_{1-x}\text{As}$.

In conclusion, we have demonstrated that a parallel magnetic field component changes the in-plane motion of a space-charge layer on GaAs from isotropic to anisotropic in the electric limit. Perpendicular to the in-plane field the reciprocal effective mass decreases with the square of the magnetic field strength due to coupling to intersubband resonances.

We would like to thank D. Heitmann and H. L. Störmer for many valuable discussions.

- ¹T. Ando, A. B. Fowler, and F. Stern, *Rev. Mod. Phys.* **54**, 437 (1982).
²J. C. Maan, Ch. Uihlein, L. L. Chang, and L. Esaki, *Solid State Commun.* **44**, 653 (1982).
³R. E. Prange and T. W. Nee, *Phys. Rev.* **168**, 779 (1968).
⁴R. E. Doezema and J. F. Koch, *Phys. Rev. B* **5**, 3866 (1972).
⁵W. Beinvoogl, A. Kamgar, and J. F. Koch, *Phys. Rev. B* **14**, 4274 (1976).
⁶T. Ando, *Phys. Rev. B* **19**, 2106 (1979).
⁷H. Schaber and R. E. Doezema, *Phys. Rev. B* **20**, 5257 (1979).
⁸J. H. Crasemann, U. Merkt, and J. P. Kotthaus, *Phys. Rev. B*

28, 2271 (1983).

⁹U. Merkt, *Phys. Rev. B* **32**, 6699 (1985).

¹⁰S. J. Allen, Jr., D. C. Tsui, and R. A. Logan, *Phys. Rev. Lett.* **38**, 980 (1977).

¹¹E. Batke, D. Heitmann, and C. W. Tu (unpublished).

¹²F. Stern, *Phys. Rev. Lett.* **18**, 546 (1968).

¹³E. Batke and D. Heitmann, *Solid State Commun.* **47**, 819 (1983).

¹⁴T. N. Theis, *Surf. Sci.* **98**, 515 (1980).

¹⁵F. Stern, *Phys. Rev. Lett.* **21**, 1687 (1968).